

# Femtosecond Laser Assisted Micro Dimple Formation on Moly-chrome film

V. Ezhilmaran<sup>1</sup>, L. Vijayaraghavan<sup>1</sup>, N. J. Vasa<sup>2</sup>, Sivarama Krishnan<sup>3</sup>

<sup>1</sup>Department of Mechanical Engineering, Indian Institute of Technology Madras, Chennai-600036, INDIA  
E-mail: me13d062@smail.iitm.ac.in

<sup>2</sup>Department of Engineering Design, Indian Institute of Technology Madras, Chennai-600036, INDIA

<sup>3</sup>Department of Physics, Indian Institute of Technology Madras, Chennai-600036, INDIA

## Abstract

Laser ablation with a pulse duration in the order of few femtoseconds (fs) is a feasible solution for texturing applications which require high quality with moderate material removal. In this present work, laser ablation of the moly-chromium film by femtosecond pulsed laser with the pulse duration of 120 fs, wavelength of 800 nm and a pulse repetition rate of 1 kHz was studied. The effect of key laser parameters, such as laser fluence and number of pulses was studied in air ambience to generate micro dimples. The ablation threshold and ablation rate for different laser energies were determined. Dimple geometries, such as diameter and depth were investigated by using scanning electron microscopy and surface profiler. As most of the absorbed energy is utilized for the ablation process, the micro-dimples produced by using femtosecond pulses exhibited a clean surface finish for lesser laser fluence and number of pulses. The increase of laser fluence and pulse numbers beyond a critical value dramatically affected the dimple surface by inducing severe cracks due to heat accumulation. So, further studies are being carried out to minimise the heat accumulation effects around the dimple processed area.

**Key words:** Ultrafast laser, heat accumulation, micro-dimple.

## 1. INTRODUCTION

Appropriate surface patterning is an important aspect in reducing friction in lubrication systems, such as piston ring-liner contacts, journal bearings and mechanical seals etc. The tribological properties of any relatively sliding surfaces can be enhanced by surface texturing, presenting the usefulness of friction and wear reduction as well as energy conservation by minimizing the mechanical loss [1]. Functionalizing a surface with micro or nanostructures is quite challenging as the structural size becomes smaller. Surface modification by using pulsed lasers is one of the most promising techniques for texturing for a number of reasons like reliability, high marking precision and cost-effectiveness. In the case of lasers with longer pulses, the material is removed by melt expulsion mechanism, in which both material vaporization and melting occurs [2].

On the other hand, texturing a surface with an ultrashort pulse laser is a fast and simple process that can be used to modify the properties of the irradiated area. It has been reported that femtosecond (fs) laser assisted material processing is a very efficient means for accurate micro/nano machining of materials due to minimal heat affected zone, clear ablation crater, and reproducibility [3]. The ablation mechanisms by a fs pulse can be classified into four divisions: normal vaporization, phase explosion, electrostatic ablation, and spallation [4]. Among them, phase explosion has been identified as the important mechanism of fs laser ablation of metals. The energy absorption at the top surface of the target is very high so direct solid to vapour transition occurs and the heat does not get dissipated out of the beam spot radius because the pulse duration is smaller than the relaxation time of electrons [5]. Due to unique ablation phenomena, the interaction between ultrashort laser pulses of femtosecond order and a material has attracted many researchers [6]. But laser interaction with a material is a bit complex process, in which many parameters play a key role. Laser beam properties, such as wavelength, pulse duration, polarization, quality factor  $M^2$  has a direct influence in the material ablation. In addition, process parameters such as the laser fluence, pulse repetition rate and pulse numbers also play a major role in deciding the quality of the ablation process [7].

When using high repetition rate in the order between few hundred kHz and MHz, the heat accumulation negatively affects the ablation quality significantly. The heat accumulation effect also strongly depends upon the laser fluence and the properties of the target material [8]. In fact, previous studies [9] have shown that for shorter pulses, less thermal energy resides in the material after the laser pulse and that heat accumulation strongly depends on the pulse energy. This heat accumulation effect causes a rapid increase in the mean temperature of the irradiated region. Therefore, heat accumulation may limit the laser ablation efficiency and the achievable precision of the ablated region. At the same time, the quality of the ablated region might be drastically reduced.

In the present study,  $Ti^{3+}:Al_2O_3$  laser with a center wavelength of 800 nm was used to produce dimple on the chromium films deposited over the cast iron piston rings. A study on the influence of laser fluence on heat accumulation effect was conducted. An experimental investigation on the relationship between the laser fluence and dimple size was carried out for various pulse numbers. The generated shape and resolution of the dimple were investigated. The threshold fluence was determined by using extrapolation method. In addition, the morphological analysis of the nanostructures on the ablated surface was conducted by scanning electron microscopy (SEM).

## 2. EXPERIMENTAL SETUP

The commercially available piston ring samples were used in the study. The ring made from the spheroidal graphite cast iron consisted of a moly-chrome thin film coating of thickness 130  $\mu m$  to resist abrasive wear. The ring has an inner diameter of 89 mm, width of 2.4 mm and thickness of 3 mm. The hardness of the moly-chrome film was measured to be 940 HV. A femtosecond pulsed  $Ti^{3+}$ :Sapphire laser (Coherent, Astrella) with a center wavelength of 800 nm, pulse repetition rate of 1 kHz and a pulse width of approximately 120 fs was used to produce dimples on the moly-chrome film. A 10-mm biconvex lens was used to focus a near-Gaussian laser beam profile. All the samples were kept at the focal position. Figure 1 shows the ring sample mounted on a rotary stage (Sigma Koki shot - Mini 5P) that was fixed

to XY translational stage. To produce dimple, the material was ablated with five different laser fluence, such as 3.7, 5.6, 8.4, 12, 16 J/cm<sup>2</sup> respectively. Every spot was ablated with pulses numbers ranging from 1000 to 12000 for each laser fluence and the dimple parameters were examined. The dimensions of the dimple were obtained using the surface profiler (Bruker, Contour GT). In order to avoid dispersion in measuring dimple diameter, two circles were drawn inside and around the dimple i.e. one is inscribed and another one is circumscribed. The average of the two circles was considered as the average dimple diameter. The average depth of the dimple was estimated by sampling at 5 different locations inside the dimple and averaged. FEI Quanta scanning electron microscopy was used to examine the quality of the ablated surface.

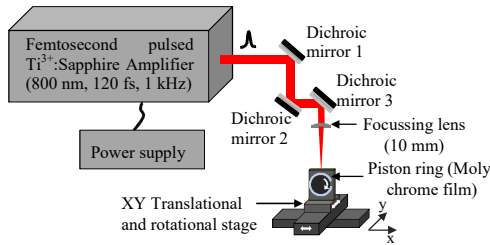
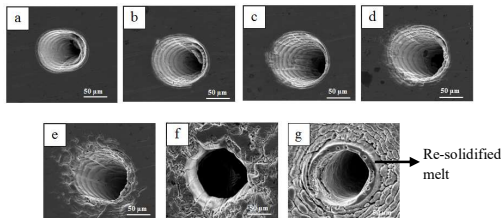


Fig. 1. Experimental setup for laser ablation

### 3. RESULTS AND DISCUSSION

#### 3.1 Influence of laser fluence and pulse numbers

Before establishing a relation between the laser fluence as well as the number of pulses with the dimple size, a preliminary investigation was conducted to figure out the suitable range of laser fluence which could offer dimple without heat effects. Different laser fluence, such as 3.7, 5.6, 8.4, 12, 16, 22.6, 28.5 J/cm<sup>2</sup> were used for the analysis. The number of pulses was fixed at 12000. Figure 2 shows the SEM image of the dimples fabricated with various laser fluence for 12000 number of pulses. As the laser fluence increased, the ablated area increased and a change in the surface morphology around the dimple was observed. At higher fluence levels of more than 8.4 J/cm<sup>2</sup>, micro-cracks were seen around the dimple. This defect was also observed with a lesser number of pulses for the laser fluence of more than 8.4 J/cm<sup>2</sup>. The magnitude of micro-cracks was severe for the laser fluence of more than 22.6 J/cm<sup>2</sup>. At a high laser fluence of 28.5 J/cm<sup>2</sup>, a ripple-like structure was clearly observed around the dimple. In addition, re-solidified



melt at the dimple edge indicated the occurrence of melting during laser irradiation. This verified that the selection of suitable laser fluence was essential to

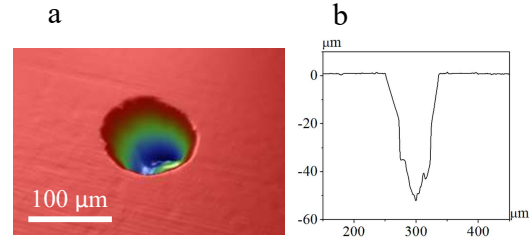


Fig. 3. (a) Typical 3D surface profiler image of the dimple and (b) the corresponding dimple profile (Dimple was fabricated with laser fluence: 8.4 J/cm<sup>2</sup>, Number of pulses: 4000).

minimize the occurrence of heat effects.

Influence of laser fluence and pulse numbers on dimple diameter and depth was then obtained by ablating the sample. Different laser fluence, such as 3.7, 5.6, 8.4, 12 and 16 J/cm<sup>2</sup>, and pulse numbers ranging from 1000 to 12000 were used for the analysis. This analysis was carried out to find the influence of laser fluence on geometrical and morphological changes in the dimple.

The three-dimensional surface profiler image of a dimple and the corresponding profile is shown in Fig. 3(a) and (b). Figure 3(b) clearly showed that the dimple surface was very clean without any burr or cracks. As the number of laser pulses increased, the ablated area gets deeper and bigger. The influence of dimple size for various laser fluence and number of pulses were measured for the dimples obtained with the fluence of

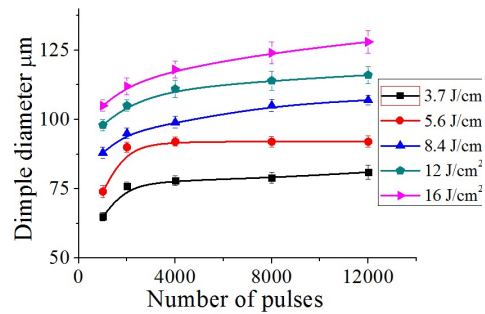


Fig. 4. Dependence of dimple diameter as a function of number of pulses for different laser fluence.

less than 16 J/cm<sup>2</sup>. The variation of dimple diameter and depth with respect to the change in laser fluence are shown in Fig. 4 and Fig. 5. At a lower laser fluence of 3.7 J/cm<sup>2</sup>, dimple diameter varied from 62 μm (1000 pulses) to 81 μm (12000 pulses) and the depth of the dimple varied from 11 μm (1000 pulses) to 70 μm (12000 pulses). Whereas, at a high laser fluence of 16 J/cm<sup>2</sup>, dimple diameter varied between 105 μm (1000 pulses) to 128 μm (12000 pulses) and the depth of the dimple varied from 34 μm (1000 pulses) to 89 μm (12000 pulses). A maximum of nearly 69% increase in dimple diameter and 200% increase in dimple depth was noticed as the laser fluence increased from 3.7 to 16 J/cm<sup>2</sup> merely for 1000 number of pulses.

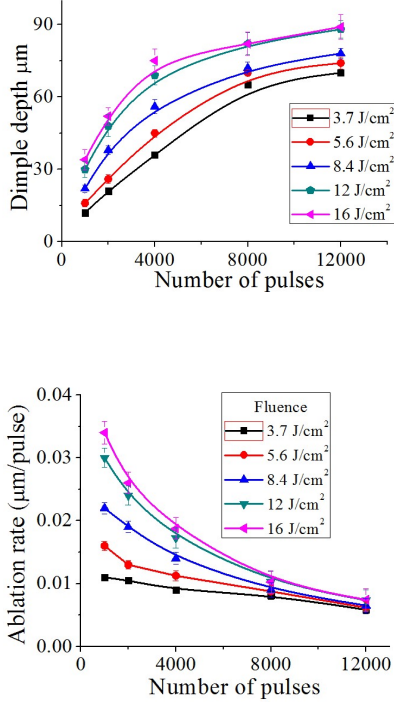


Fig. 6. Ablation rate as a function of number of pulses.

**Table 1**  
Ablation rate for first 1000 number of pulses.

Fluence (J/cm <sup>2</sup> )	Ablation rate (μm/pulse)
3.7	0.011
5.6	0.016
8.4	0.022
12	0.030
16	0.034

Figure 6 shows the ablation rate of the target material for the various laser fluence and number of pulses. Laser pulses with a high fluence of 16 J/cm<sup>2</sup> showed a high ablation rate compared to the other lower fluence considered for the analysis. Also, the ablation rate was high with 1000 number of pulses. The ablation rate decreased with the increase of number of pulses. A minimum ablation rate was observed for 12000 number of pulses. The ablation rate for the different laser fluence and with 1000 number of pulses is shown in Table 1. The ablation rate for the lesser laser fluence of 3.7 J/cm<sup>2</sup> was 0.011 μm/pulse whereas, for the laser fluence of 16 J/cm<sup>2</sup>, a high ablation rate of 0.034 μm/pulse was observed. Hence, it was verified that the material removal mainly took place during the initial ablation time period and it gradually decreased with the increase of time.

### 3.2 Ablation threshold

The ablation threshold of any material during laser processing plays a prominent role in deciding the physical mechanism of the interaction between the laser beam and the target surface [10]. The ablation threshold refers to the critical laser fluence of the incident laser pulse for the material being ablated. A common method to find the ablation threshold is by extrapolation [11, 12], whereby the value of any one of ablation volume

diameter and depth of 0 is extrapolated from the linear relationship curve of the ablation volume or diameter and laser fluence to estimate the ablation threshold. Figure 7 shows the dimple diameter plot obtained with different laser fluence (Number of pulses = 1000). The dimple diameter decreased with the decrease of fluence and reached a minimum value at 3.7 J/cm<sup>2</sup>. The threshold laser fluence after extrapolating the curve was estimated approximately as 0.3 to 0.5 J/cm<sup>2</sup>. Figure 8 shows the dimple depth plot obtained with different laser fluence (Number of pulses = 1000). The dimple depth reached zero at the laser fluence ranging between 0.3 to 0.5 J/cm<sup>2</sup>, which was the same as that of the threshold fluence value obtained by using dimple diameter extrapolation. The ablation threshold in the case of ultrashort pulsed laser can be obtained numerically by using,

$$L_d = \alpha^{-1} \ln\left(\frac{F_a}{F_{th}}\right)$$

Where,  $L_d$  is the ablation depth per pulse (0.012 μm/pulse),  $\alpha$  is the absorption coefficient ( $\alpha = 5.4359 \times 10^5 \text{ cm}^{-1}$  for chromium),  $F_a$  is the applied

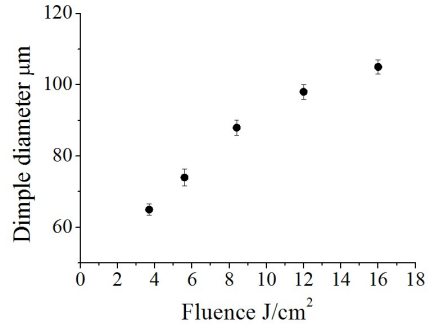
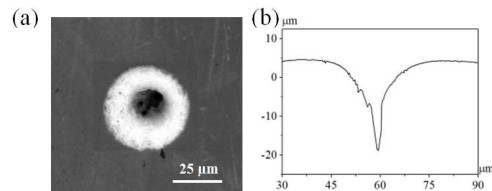
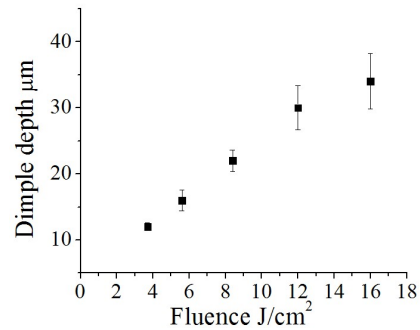


Fig. 7. Relationship between dimple diameter and laser fluence for 1000 number of pulses.



laser fluence ( $3.7 \text{ J/cm}^2$ ),  $F_{th}$  is the ablation threshold fluence. The ablation threshold fluence was estimated to be around  $0.8 \text{ J/cm}^2$ . This numerically estimated value is in close agreement with the experimental value.

Figure 9(a) shows the dimple fabricated at the fluence nearer to the ablation threshold (i.e.  $1.5 \text{ J/cm}^2$ ) with 12000 number of pulses. The dimple was free from heat effects and debris. But the ripple-like structure was present inside the dimple surface. In addition, minute holes were present at the bottom of the dimple surface. The corresponding dimple profile showed that the dimple was narrow towards the depth and wide at the edges. Further studies are being carried out to study the geometrical and morphological characteristics of the dimples at near threshold ablation fluence.

### 3.3 Dimple morphology study

The dimples were obviously almost circular. There were many burrs and broken holes in some of the dimples. It can be assumed that incubation effects combined with increased laser absorption at the surface lead to the formation of burr at fluence above ablation threshold [13]. Many ripple patterns of lower magnitude were observed inside the dimple surface fabricated at lesser fluence (Fluence  $< 16 \text{ J/cm}^2$ ) as shown in Fig. 2(a-e). This is attributed to normal vaporization along lines of constructive interference, which arise when the incident beam interferes with a scattered tangential wave [14]. The ripple pattern usually formed early during laser ablation, provides a sinusoidal corrugation, which acts as a grating for next incoming pulses thus increased ripple growth [12, 14]. In addition, at a higher frequency of 1 kHz, free ionization electrons are subjected to vibration, which is not conducive to electronic ionization and acceleration [12]. Recently, some researchers proposed that the interaction between the incident laser light and the excited surface plasma (SP) wave is responsible for the formation of ripples induced by femtosecond pulsed lasers on a metal surface [15]. A high magnitude of heat effects was seen around the dimple circumference fabricated at laser fluence of  $22.6 \text{ J/cm}^2$  and  $28.5 \text{ J/cm}^2$  (Fig. 2 (f & g)). The SEM images showed a proof of melting adjacent to the ripple patterns. This clearly verifies that vaporization along with melting is the main phenomena responsible for removal of material at high laser fluence.

### 3.4 SEM analysis

The EDS analysis was carried out at 4 different places, such as at the base material (Spot 1), at the surface outside the dimple where no heat effects were observed (Spot 2), at the heat affected area around the dimple (Spot 3) and inside the dimple (Spot 4) as shown in Fig. 10 (a). The common elements present in all the spots were Cr, Mo, Mn, C and O, respectively as shown in Table 1. At the EDS spot 1, the presence of Cr (94%) was high and the remaining elemental composition is given as C-2%, O-1%, Mo-0.5 and Mn- 1.1%. The carbon and oxygen composition was little increased near to the dimple location. At EDS spot 2, the chromium percentage was decreased to 83% and the remaining elemental composition is given as C-7%, O-6%, Mo-0.8% and Mn-1.4%. The results indicated a significant increase of carbon and oxygen percentage was observed near to the dimple edge. The magnified view around the dimple edge indicated the presence of cracks as minute particles. At the EDS spot 3 and 4 that is located at the

dimple edge and inside the dimple, the chromium percentage was decreased to 54% and 39%. A significant increase in carbon and oxygen was observed. The presence of oxygen might influence the change in absorption coefficient of the material which in turn modifies the temperature field and material properties [16]. Hence, further analysis is carried out to minimize the formation of oxide in the laser irradiated region. The magnified view at the dimple edge (Fig. 10(b)) shows the presence of micro cracks. The presence of micro-crack will affect the functional efficiency of the material. This can be reduced by ablating the material at near ablation threshold.

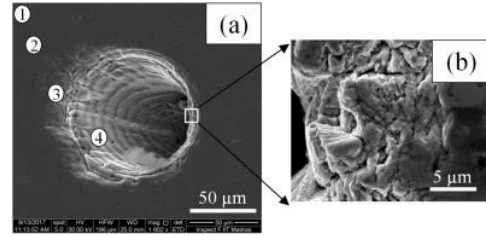


Fig. 10 (a). EDS analysis at the dimple (Fluence of  $8.4 \text{ J/cm}^2$  and 4000 number of pulses) and (b) The magnified view of the dimple edge.

Table 1: EDAX analysis at various dimple locations.

Sample location	Elements weight percentage (%)				
	Cr	C	O	Mn	Mo
Region 1	94	2	1	0.5	1.1
Region 2	83	7	6	0.8	1.4
Region 3	53	31	12	1.2	1.7
Region 4	39	30	27	1.5	1.7

## 4 CONCLUSION

The present study showed that the ablation quality was significantly influenced by laser parameters. Dimple surface was very rough when the material was ablated at high laser fluence. The variation in dimple sizes both the diameter and depth was measured as a function of laser fluence and pulse numbers. The increase in both laser fluence and number of pulses increased the dimple size to a large extent. A maximum of nearly 69% and 200% increase in dimple diameter and depth was noted as the laser fluence increased from  $3.7$  to  $12 \text{ J/cm}^2$  for 1000 number of pulses. A high ablation rate was observed for a high fluence of  $16 \text{ J/cm}^2$  ( $0.03 \text{ µm/pulse}$ ) during the initial period of ablation. Multiple shot ablation threshold for the molybdenum-chrome film was estimated to be in the range of  $0.3$  to  $0.5 \text{ J/cm}^2$ .

### Acknowledgement

The authors are grateful to MEMS lab and SEM lab for the technical support. The authors would like to thank Dr. Mahadevan from India pistons limited for his continuous support. The research work is partially supported by the DST-AMT Program (DST/TSG/AMT/2015/353).

### References

- [1] W. Wu, G. Chen, B. Fan, J. Liu, Effect of groove surface texture on tribological characteristics and energy consumption under high temperature friction, PloS one, 11 (2016) e0152100.

- [2] W. Schulz, U. Eppelt, R. Poprawe, Review on laser drilling I. Fundamentals, modeling, and simulation, *Journal of Laser Applications*, **25** (2013) 012006.
- [3] D.J. Hwang, H. Jeon, C.P. Grigoropoulos, J. Yoo, R.E. Russo, Femtosecond laser ablation induced plasma characteristics from submicron craters in thin metal film, *Applied Physics Letters*, **91** (2007) 251118.
- [4] T.E. Itina, F. Vidal, P. Delaporte, M. Sentis, Numerical study of ultra-short laser ablation of metals and of laser plume dynamics, *Applied Physics A*, **79** (2004) 1089-1092.
- [5] S. Mishra, V. Yadava, Laser beam micromachining (LBMM)—a review, *Optics and lasers in engineering*, **73** (2015) 89-122.
- [6] J. Cheng, C.-s. Liu, S. Shang, D. Liu, W. Perrie, G. Dearden, K. Watkins, A review of ultrafast laser materials micromachining, *Optics & Laser Technology*, **46** (2013) 88-102.
- [7] B.K. Nayak, M.C. Gupta, Self-organized micro/nano structures in metal surfaces by ultrafast laser irradiation, *Optics and Lasers in Engineering*, **48** (2010) 940-949.
- [8] A. Ancona, S. Döring, C. Jauregui, F. Röser, J. Limpert, S. Nolte, A. Tünnermann, Femtosecond and picosecond laser drilling of metals at high repetition rates and average powers, *Optics letters*, **34** (2009) 3304-3306.
- [9] J. Yang, Y. Zhao, X. Zhu, Transition between nonthermal and thermal ablation of metallic targets under the strike of high-fluence ultrashort laser pulses, *Applied physics letters*, **88** (2006) 094101.
- [10] P.T. Mannion, J. Magee, E. Coyne, G.M. O'Connor, T.J. Glynn, The effect of damage accumulation behaviour on ablation thresholds and damage morphology in ultrafast laser micro-machining of common metals in air, *Applied Surface Science*, **233** (2004) 275-287.
- [11] S. Banerjee, R. Fedosejevs, Single-shot ablation threshold of chromium using UV femtosecond laser pulses, *Applied Physics A*, **117** (2014) 1473-1478.
- [12] B. Zheng, G. Jiang, W. Wang, K. Wang, X. Mei, Ablation experiment and threshold calculation of titanium alloy irradiated by ultra-fast pulse laser, *AIP Advances*, **4** (2014) 031310.
- [13] K.-H. Leitz, B. Redlingshöfer, Y. Reg, A. Otto, M. Schmidt, Metal Ablation with Short and Ultrashort Laser Pulses, *Physics Procedia*, **12** (2011) 230-238.
- [14] P. Mannion, J. Magee, E. Coyne, G. O'connor, T. Glynn, The effect of damage accumulation behaviour on ablation thresholds and damage morphology in ultrafast laser micro-machining of common metals in air, *Applied surface science*, **233** (2004) 275-287.
- [15] M. Huang, F. Zhao, Y. Cheng, N. Xu, Z. Xu, Origin of laser-induced near-subwavelength ripples: interference between surface plasmons and incident laser, *ACS nano*, **3** (2009) 4062-4070.
- [16] I. Iordanova, V. Antonov, Surface oxidation of low carbon steel during laser treatment, its dependence on the initial microstructure and influence on the laser energy absorption, *Thin Solid Films*, **516** (2008) 7475-7481.